

# Reconstruction of photon-number distribution using low-performance photon counters

Guido Zambra<sup>1,2</sup> and Matteo G. A. Paris<sup>1</sup>

<sup>1</sup>*Dipartimento di Fisica dell'Università di Milano, Milan, Italy*

<sup>2</sup>*Dipartimento di Fisica e Matematica dell'Università degli Studi dell'Insubria, Como, Italy*

(Received 6 July 2006; published 27 December 2006)

The output of a photodetector consists of a current pulse whose charge has the statistical distribution of the actual photon numbers convolved with a Bernoulli distribution. Photodetectors are characterized by a nonunit quantum efficiency, i.e., not all the photons lead to a charge, and by a finite resolution, i.e., a different number of detected photons leads to a discriminable values of the charge only up to a maximum value. We present a detailed comparison, based on Monte Carlo simulated experiments and real data, among the performances of detectors with different upper limits of counting capability. In our scheme the inversion of Bernoulli convolution is performed by maximum-likelihood methods assisted by measurements taken at different quantum efficiencies. We show that detectors that are only able to discriminate between zero, one and more than one detected photons are generally enough to provide a reliable reconstruction of the photon number distribution for single-peaked distributions, while detectors with higher resolution limits do not lead to further improvements. In addition, we demonstrate that, for semiclassical states, even on/off detectors are enough to provide a good reconstruction. Finally, we show that a reliable reconstruction of multi peaked distributions requires either higher quantum efficiency or higher resolution.

DOI: [10.1103/PhysRevA.74.063830](https://doi.org/10.1103/PhysRevA.74.063830)

PACS number(s): 42.50.Ar, 03.65.Wj, 85.60.Gz

## I. INTRODUCTION

Reconstruction of the photon number distribution,  $\varrho_n$ , of optical states provides fundamental information on the nature of any light beam and finds relevant applications in quantum mechanics, quantum state engineering by postselection [1], quantum information [2], and quantum metrology. However, despite the relevant applications in the above fields, photon detectors that can operate as photon counters [3,4] for any state of radiation are still rather rare [5]. Among these, photomultiplier tubes (PMT's) [6] and hybrid photodetectors [4,7] are promising devices, though they have the drawback of a low quantum efficiency. On the other hand, solid state detectors with internal gain, which ensures higher efficiency, are still under development. Highly efficient thermal detectors have also been used as photon counters, though their operating conditions are still extreme to allow common use [8,9]. Quantum tomography also provides an alternative method to measure photon number distributions [10,11], but this method needs the implementation of homodyne detection, which in turn requires the appropriate mode matching of the signal with a suitable local oscillator at a beam splitter, a challenging task in the case of pulsed optical fields.

In principle, in a photodetector each photon ionize a single atom, and the resulting charge is amplified to produce a measurable pulse. In practice, however, the performances of real photodetectors are affected by two main limitations: nonunit quantum efficiency and imperfect counting capability, i.e., finite resolution. A quantum efficiency smaller than unity means that only a fraction of the incoming photons leads to an electric pulse. If the resulting current is proportional to the incoming photon flux we have a linear photodetector. This is, for example, the case of the high-flux photodetectors used in homodyne detection. On the other hand, photodetectors operating at very low intensities usually resort to avalanche process or very high amplification in order

to transform a single ionization event into a recordable pulse. Since each charge is independently amplified, overall we have a gain instability in the amplification process, which is, in turn, affected by a total noise that is much larger than that of a single event. As soon as the light flux increases, linearity is lost on the single event, and the resulting noise makes very difficult to discriminate the number of detected photons.

Overall, we have that the output of a photodetector consists of a current pulse whose charge statistics is a generalized Bernoulli convolution of the actual photon distribution [12]. In addition, the discrimination between the number of detected photons is only possible up to a finite number. We refer to the maximum number  $m$  of detected photons that can be distinguished from  $m-1$  as the resolution  $M$ , which represents the maximum counting capability of the detector. Detectors that works in Geiger mode have  $M=1$  because from the output is possible to discriminate from  $m=1$ , one detected photon, to  $m=0$ , dark, but is not possible to discriminate the output for  $m \geq 2$  from that for  $m=1$ .

Reconstruction of the photon number distribution from the output of a realistic photodetector requires the inversion of the Bernoulli convolution. Even in principle, this task is not always possible [13]. As for example, for truly infinite distributions it is possible only for quantum efficiency for larger than  $\eta=0.5$  [14]. For truncated distribution it is possible for any value of the efficiency, but it is inherently ineffective, as it requires a large data sample to provide a reliable result. On the other hand, maximum-likelihood methods assisted by measurements taken at different quantum efficiencies have been proved to be both effective and statistically reliable [13,15–17]. In particular, it is possible to obtain a method to reconstruct  $\varrho_n$  without any *a priori* information on the state of light under investigation. An alternative approach is based on the so-called *photon chopping* [18], i.e., on a network of beam splitter followed by an array of on/off detectors. Photon chopping allows to send at most one photon

on each detector, however, with the drawback of increasing the overall complexity of the detection scheme.

In this paper, we extend a previous analysis based on maximum-likelihood on/off schemes [13,16], and carry out comparison among the performances of detectors characterized by realistic quantum efficiencies and different values of the resolution  $M$ . The comparison is made using real data and by an extensive set of Monte Carlo simulations, performed on different states of the radiation field including quantum and semiclassical states associated to single peaked as well as multi-peaked photon distributions. The reconstruction is obtained by maximum-likelihood methods assisted by measurements taken at different quantum efficiencies. In particular, as the statistics of the detected photons is linearly dependent on the photon distribution (see below), the inversion can be performed by means of the expectation-maximization (EM) algorithm which leads to an effective and reliable iterative solution.

Our results indicate that detectors with resolution  $M=2$ , i.e., discriminating between zero, one and more than one photon, are generally enough to provide a reliable reconstruction of the photon number distribution for single-peaked distributions, while detectors with higher value of  $M$  do not lead to further improvements. On the other hand, multi-peaked distributions requires a higher quantum efficiency, whereas for semiclassical states even on/off detectors are enough to provide a good reconstruction.

The paper is structured as follows. In the next section we describe the statistics of the detected photons and illustrate the reconstruction algorithm. In Sec. III we report the results of a set of Monte Carlo simulated experiments performed on different kinds of signals, whereas in Sec. IV we report experimental results for coherent signals. Section. V closes the paper with some concluding remarks.

## II. STATISTICS OF DETECTED PHOTONS AND RECONSTRUCTION ALGORITHM

Using a photodetector with quantum efficiency  $\eta$  and unbounded resolution ( $M=\infty$ ), i.e., unlimited counting capability, the probability of obtaining  $m$  detected photons at the output is given by the convolution [12]

$$p_\eta(m) = \sum_{n=m}^{\infty} A_\eta(m,n) \varrho_n, \quad (1)$$

where  $\varrho_n = \langle n | \varrho | n \rangle$  is the actual photon number distribution of the signal under investigation, i.e., the expectation values of the projectors over Fock state,  $\varrho$  being the density operator of the mode. The matrix  $A_\eta(m,n)$  is given by

$$A_\eta(m,n) = \binom{n}{m} (1-\eta)^{n-m} \eta^m. \quad (2)$$

If  $M$  has a finite value, then only  $M+1$  outcomes are possible, which occur with probabilities

$$q_\eta^m = p_\eta(m), \quad m = 0, \dots, M-1, \quad (3)$$

$$q_\eta^M = \sum_{m=M}^{\infty} p_\eta(m) = 1 - \sum_{m=0}^{M-1} q_\eta^m. \quad (4)$$

Once the value of the quantum efficiency is known, Eqs. (3) and (4) provide  $M+1$  relations ( $M$  independent relations) among the statistics of detected photons and the actual statistics of photons. At first sight the statistics of a detector with low counting capability ( $M$  in the range  $M=1, \dots, 6$ ) appears to provide quite a scarce piece of information about the state under investigation. However, if the distribution of detected photons  $\{q_\eta^m\}$  is collected for a suitably large set of  $\eta$ , then the information is enough to reconstruct the whole photon distribution  $\varrho_n$  of the signal, upon a suitable truncation at  $N$  of the Hilbert space. We adopt the following strategy: by placing in front of the detector  $K$  filters with different transmissions, we may perform the detection with  $K$  different values  $\eta_\nu$ ,  $\nu=1, \dots, K$ , ranging from a minimum value  $\eta_1$  to a maximum value  $\eta_K = \eta_{\max}$  equal to the nominal quantum efficiency of the detector. By denoting the probability of having  $m$  detected photons in the experiment with quantum efficiency  $\eta = \eta_\nu$ , by  $q_\nu^m \equiv q_\eta^m$  we can rewrite Eqs. (3) and (1) as

$$q_\nu^m[\{\varrho_n\}] = \sum_{n=m}^{\infty} A_\nu(m,n) \varrho_n, \quad (5)$$

where  $\nu=1, \dots, K$  and  $m=0, \dots, M-1$ . Let us now suppose that the  $\varrho_n$ 's are negligible for  $n > N$  and that the  $\eta_\nu$ 's are known, then  $\forall \eta_\nu$  Eq. (5) may be rewritten as a finite sum over  $n$  from  $m$  to  $N$ . Overall, we obtain a finite linear system with  $K \times M$  equations in the  $N+1$  unknowns  $\{\varrho_n\}$ . Unfortunately, the reconstruction of  $\varrho_n$  by matrix inversion cannot be used in practice since it would require an unreasonable number of experimental runs to assure the necessary precision [13,15]. This problem can be circumvented by considering Eqs. (5) as a statistical model for the parameters  $\{\varrho_n\}$  to be solved by maximum-likelihood (ML) estimation. The likelihood functional is given by the global renormalized probability [19] of the sample, i.e.,

$$\mathcal{L} = \prod_{\nu=1}^K \prod_{m=0}^{M-1} \left( \frac{q_\nu^m}{\sum_{\lambda} q_\nu^\lambda} \right)^{n_{m\nu}}. \quad (6)$$

The ML estimates of  $\{\varrho_n\}$  are the values that maximizes  $\mathcal{L}$ . In Eq. (6)  $n_{m\nu}$  denotes the number of “ $m$  detected photons” events obtained with quantum efficiency  $\eta_\nu$ . The maximization of  $\mathcal{L}$  under the constraints  $\varrho_n \geq 0$ ,  $\sum_n \varrho_n = 1$ , can be obtained by using the expectation-maximization algorithm [20–22], which leads to the iterative solution

$$\begin{aligned} \varrho_n^{(i+1)} &= \varrho_n^{(i)} \left( \sum_{\nu=1}^K \sum_{m=0}^{M-1} A_\nu(m,n) \right)^{-1} \\ &\times \sum_{\nu=1}^K \sum_{m=0}^{M-1} A_\nu(m,n) \frac{f_\nu^m}{q_\nu^m[\{\varrho_n^{(i)}\}]}. \end{aligned} \quad (7)$$

In Eq. (7)  $\varrho_n^{(i)}$  denotes the  $n$ th element of reconstructed distribution at the  $i$ th step,  $q_\nu^m[\{\varrho_n^{(i)}\}]$  the theoretical probabilities as calculated from Eq. (5) at the  $i$ th step, whereas

$f_v^m = n_{mv}/n_v$  represents the frequency of the “ $m$  detected photons” event with quantum efficiency  $\eta_v$ , being  $n_v$  the total number of runs performed with  $\eta = \eta_v$ . In the following we assume that the number of runs  $n_v$  is the same for all the  $\eta_v$ 's.

Equation (7) provides a solution once an initial distribution is chosen. In the following we will always consider an initial uniform distribution  $\varrho_n^{(0)} = (1+N)^{-1} \forall n$  in the truncated Fock space  $n=0, \dots, N$ . Results from Monte Carlo simulated experiments show that any other distribution with  $\varrho_n^{(0)} \neq 0 \forall n$  performs equally well, i.e., the choice of the initial distribution does not alter the quality of reconstruction, though it may slightly affect the convergence properties of the algorithm.

A question may arise about the choice of the cutoff  $N$ , above which the  $\varrho_n$ 's can be neglected. This, of course, depends on the average number of photons of the state under investigation, which is unknown or only partially known. An effective method to circumvent this problem is to choose a large value for  $N$  and then decreasing it (in order to decrease the number of free parameters) until the normalization condition  $\sum_n^N \varrho_n = 1$  holds within a certain precision. Results from Monte Carlo simulated experiments and from the analysis of experimental data confirm the effectiveness of this procedure, i.e., the independence of the reconstruction on the value of  $N$  (as far as  $N$  is large enough to assure normalization).

### III. MONTE CARLO SIMULATED EXPERIMENTS

In this section we report the photon number distribution for different states of a single-mode radiation field as obtained by ML reconstruction from Monte Carlo simulated photodetection performed with the same (low) quantum efficiency and different values of  $M$ . We consider semiclassical states as well as highly nonclassical states and show results for different values of the maximal quantum efficiency  $\eta_{\max}$ .

In order to assess our results and to measure the reliability and the accuracy of the method we introduce two figures of merit. Since the solution of the ML estimation is obtained iteratively, the most important aspect to keep under control is the convergence of the algorithm. A suitable parameter to evaluate the degree of convergence at the  $i$ th iteration is, besides the value of the likelihood itself, the total absolute error,

$$\varepsilon^{(i)} = \sum_{\nu=1}^K \sum_{m=0}^{M-1} |f_v^m - q_v^m[\{\varrho_n^{(i)}\}]|. \quad (8)$$

Indeed, the total error measures the distance of the probabilities  $q_v^m[\{\varrho_n^{(i)}\}]$ , as calculated at the  $i$ th iteration, from the actual experimental frequencies and thus, besides convergence, it quantifies how well the estimated distribution reproduces the experimental data [23]. The total distance is a decreasing function of the number of iterations and its stationary value is proportional to the accuracy of the experimental frequencies  $\{f_v^m\}$ . For finite data sample this value is of order  $1/\sqrt{n_v}$  for each value of  $\eta_v$ .

As a measure of the accuracy at the  $i$ th iteration we adopt the so-called fidelity between probability distributions

$$G^{(i)} = \sum_{n=0}^N \sqrt{\varrho_n^{(i)} \varrho_n}, \quad (9)$$

where  $\varrho_n$  is the actual photon number distribution and  $\varrho_n^{(i)}$  the estimated one at the  $i$  iteration. In Ref. [16] it was shown that using on/off detection (i.e.,  $M=1$ ) a reliable reconstruction scheme may be obtained. In this paper, our aim is to check whether a higher value of  $M$  leads to some advantages, either in terms of accuracy or convergence.

Figure 1 summarizes results for different states and values of  $M$ , assuming  $\eta_{\max}=0.2$  as the maximum value of the quantum efficiency. In order to compare the performances achievable by different  $M$  one must first choose a criterion to stop the iterative algorithm. A natural criterion would be that of stopping the iteration when the total absolute error  $\varepsilon^{(i)}$  converges, i.e., when the rate of its variation falls below a threshold and becomes negligible. This is also motivated by the behavior of  $\varepsilon^{(i)}$  versus the number of iterations (see central column in Fig. 1): a rapid fall followed by a plateau. However, the most convenient value for the threshold unavoidably depends on the shape of the unknown distribution  $\varrho_n$ . Therefore, assuming no *a priori* information, this threshold criterion should be supplemented by some additional recipes. We found numerically that a suitable criterion, valid for any value of  $M$  and, on the average, for any class of states, is the following: if the total absolute error appears to converge, then stop the algorithm at a number of iterations  $i_{\max} \equiv I = n_v$  equal to the number of measurements taken at each value of the quantum efficiency, otherwise stop the algorithm as soon as one sees convergence. In cases in which  $\varepsilon^{(i)}$  converges for a number of iteration  $I < n_v$ , it is not convenient to stop the algorithm, since it may further increase the quality of the reconstruction, see, for example,  $G^{(i)}$  in the fourth line of Fig. 1. On the other hand, if  $I$  goes far beyond the condition of convergence of  $\varepsilon^{(i)}$ , then the algorithm may lose in precision due to the noise of the data  $f_v^m$  (see inset in the second line of Fig. 1). The choice of the threshold at  $I = n_v$  fits with other two independent facts. On the one hand, we performed an extensive set of simulations and no considerable reduction of  $G^{(i)}$  was observed before the convergence condition  $I = n_v$ . On the other hand, we applied the reconstruction algorithm to the *exact* on/off frequencies (not to simulated data) and no reduction of  $G^{(i)}$  was observed for increasing  $I$ , thus confirming the data-noise origin of precision loss.

Let us now illustrate our results about the accuracy of the reconstructions. We have performed simulated experiments on semiclassical states like coherent and thermal ones, as well as on highly nonclassical states such as Fock states. For this simulation we used three values for the maximum quantum efficiency  $\eta_{\max}=0.2, 0.5, 0.8$ . Simulations have been performed by using  $n_v=10^4$  data at each value of the quantum efficiency. This value of  $n_v$  is relatively small and well within the realm of quantum optical experiments. In a real experiment performed under the same conditions, a value of  $n_v$  of this order would allow on-line reconstruction of the photon number distribution. Simulations performed using different values of the parameters lead to similar conclusion.

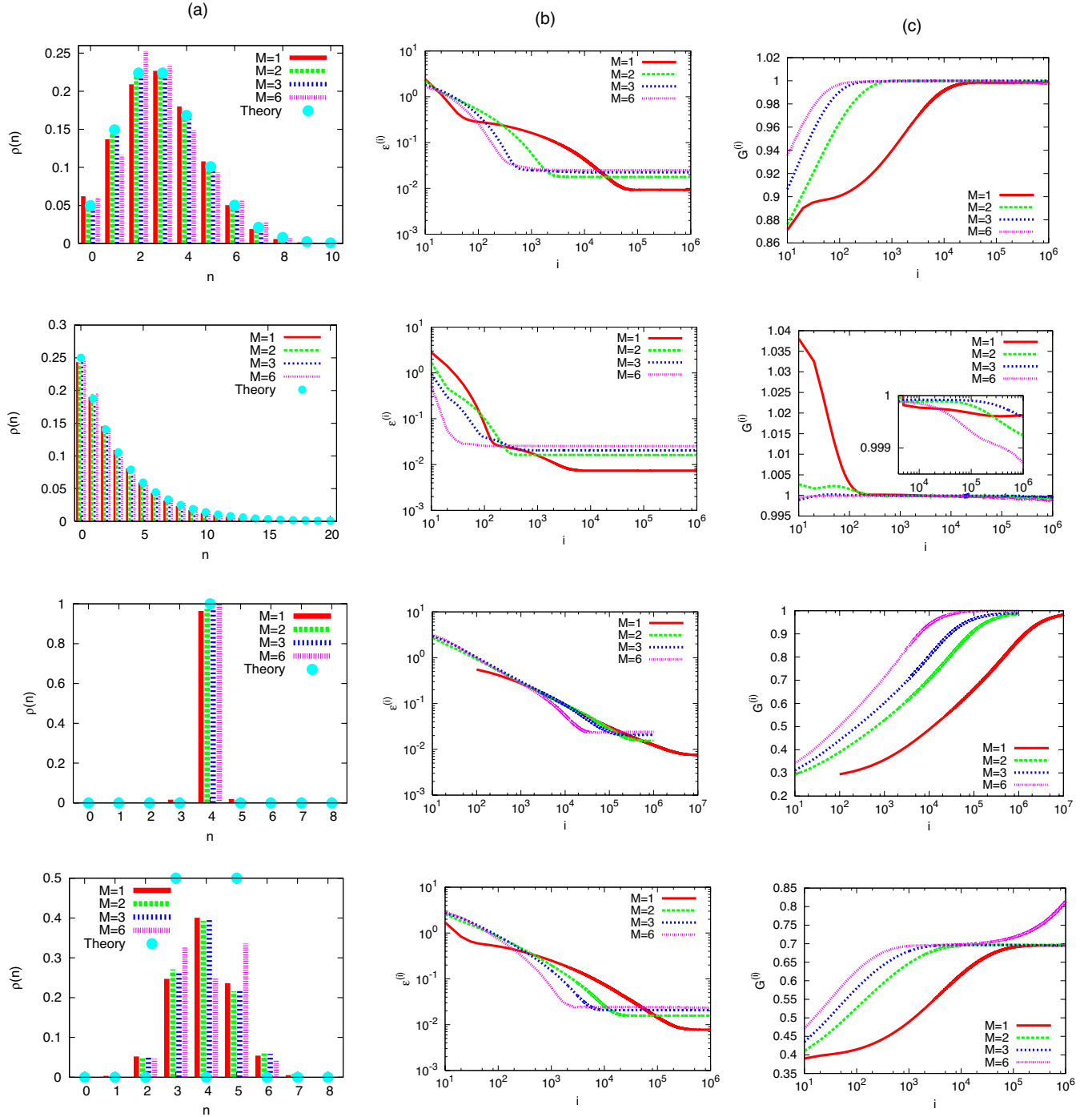


FIG. 1. (Color online) Maximum-likelihood reconstruction of photon number distribution using photodetectors with different counting capability (different values of  $M$ ) and maximum quantum efficiency  $\eta_{\max}=0.2$ . First line, photon distribution of a coherent state with  $\langle a^\dagger a \rangle=3$ ; panel (a) the reconstructed  $\rho_n$ ; (b) total absolute error  $\varepsilon^{(i)}$  according to Eq. (8); (c) fidelity  $G^{(i)}$  according to Eq. (9). Results are reported for  $M=1$  (on/off detector),  $M=2$ ,  $M=3$ , and  $M=6$ . We use  $K=30$  different quantum efficiency values  $\eta=\eta_\nu$ , uniformly distributed in  $[\eta_{\max}/K, \eta_{\max}]$ . The Hilbert space have been truncated at  $N=30$  and  $n_\nu=10^6$  runs have been performed for each value  $\eta_\nu$ . The last iteration is  $I=n_\nu$  except for the Fock state,  $M=1$ , for which  $I=10^7$ . Other lines, same as first line for thermal state with  $\langle a^\dagger a \rangle=3$ , Fock state with  $n=4$ ; superposition of two Fock states  $\frac{1}{2}(|3\rangle+|5\rangle)$ . The inset of panel (c) in the third line shows the last iterations  $i$  in an expanded scale.

In Fig. 2 we show the fidelity of reconstruction  $G^{(i)}$  at the last iterations,  $G^{(I)}$ , for different input signals and different values of  $M$  as a function of the average number of photons of the signal. As it is apparent from the plots, for low quantum efficiency and semiclassical states on/off detec-

tors ( $M=1$ ) are enough to achieve a good reconstruction. On the other hand, the accuracy for nonclassical states largely improves for  $M \geq 2$ . For higher values of the quantum efficiency (the middle and the right plots) on/off detectors become sufficient for a good reconstruction also for nonclassi-



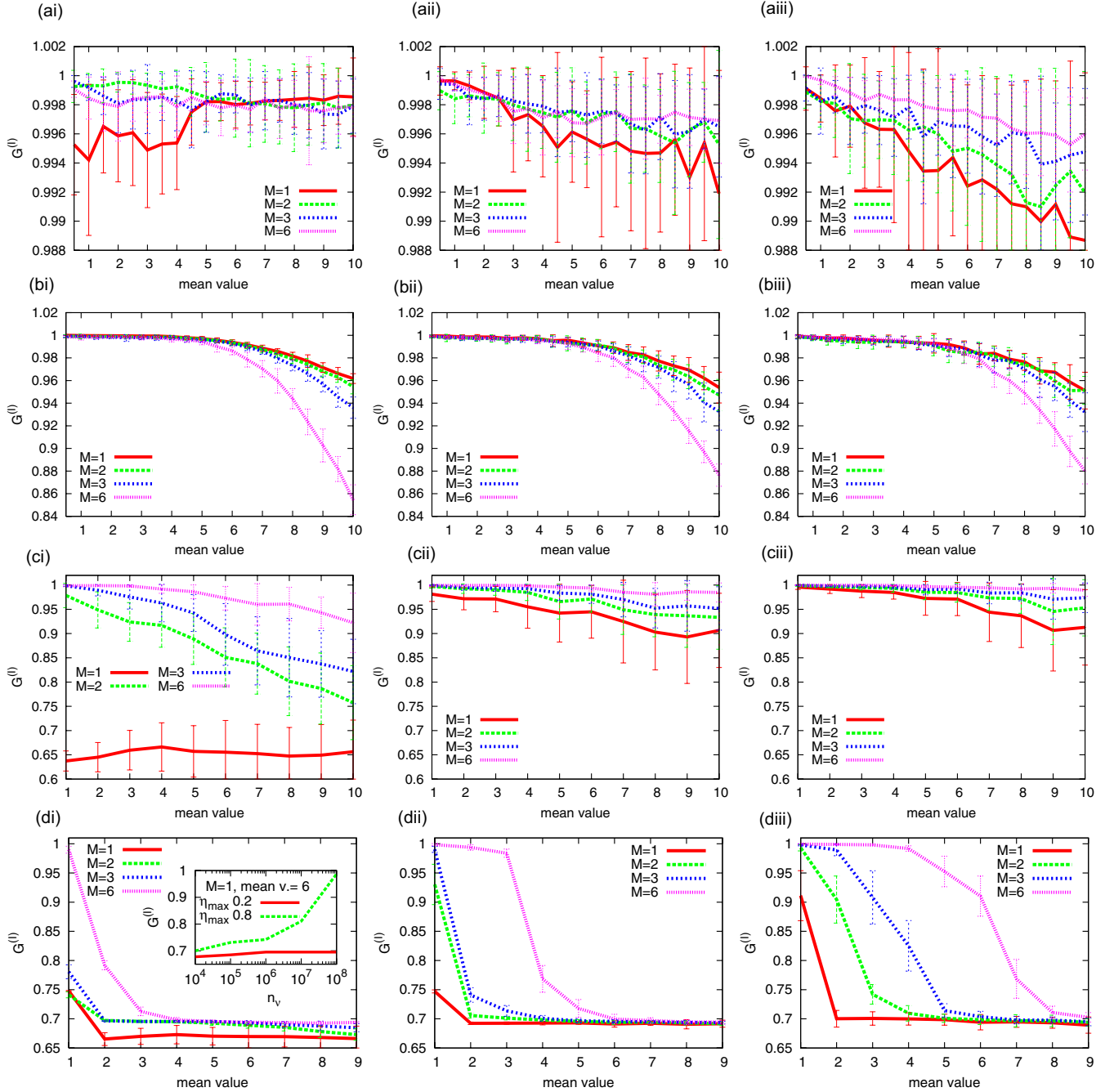


FIG. 2. (Color online) Fidelity parameter at the last iteration,  $G^{(l)}$ , as a function of  $\langle a^\dagger a \rangle$  for four different statistics of  $\{\mathcal{Q}_n\}$ : coherent, panels labeled (a); thermal, label (b); Fock state, label (c); superposition of two Fock states,  $\frac{1}{\sqrt{2}}(|\langle a^\dagger a \rangle - 1\rangle + |\langle a^\dagger a \rangle + 1\rangle)$ , label (d). The reconstructions have been performed using  $\eta_{\max}=0.2, 0.5$ , and  $0.8$ , panels labeled with (i), (ii) and (iii), respectively. Number of runs,  $n_\nu = 10^4$ . According to the rule given in the text, the last iteration performed is  $I=n_\nu$  except for the coherent state with  $\langle a^\dagger a \rangle=1$  to 4 for which  $I=10^5$  (only for  $M=1$ ), and for the superpositions state. Inset of (di) show  $G^{(l)}$  for the superposition  $\frac{1}{\sqrt{2}}(|5\rangle + |7\rangle)$ ,  $M=1$ , quantum efficiencies  $\eta=0.2$  and  $\eta=0.8$  as a function of  $n_\nu$ . Each point of the curves is the mean of 40 simulations, the error bars represent the standard deviations. The other parameters are the same as in Fig. 1.

cal states having single-peaked distributions. Notice that a higher resolution, however with a low value of  $\eta_{\max}$ , does not guarantee a good reconstruction. Also notice that the results reported in Fig. 2 has been obtained by stopping the algorithm according to the prescriptions mentioned above. We therefore do not expect that the fidelity is optimal for *any* state. Indeed, the fidelity  $G^{(l)}$  in panels (cii) and (ciii) of Fig.

2 slightly decreases for a high number of photons, though it remains close to unit value. The decreases in panels (bi), (bii), and (biii) of Fig. 2 for large mean values are due to the choice of a small dimension of the truncated Hilbert space: by increasing  $N$  this trend disappears. On the other hand, the low values of  $G^{(l)}$  for the superposition states are due to the noise in  $f_\nu^m$ . Indeed, by increasing  $n_\nu$  the reconstructions

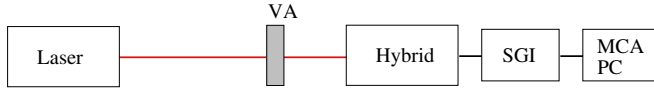


FIG. 3. (Color online) Experimental setup for reconstruction the photon number distribution of a coherent state. The laser and the detector (named hybrid) are described in the text. VA is a variable attenuator; SGI is a synchronous gated integrator; MCA is a multi-channel analyzer.

greatly improves. Moreover, for high quantum efficiency the detectors perform good reconstructions also for  $M=1$ , see the inset of panel (di) in Fig. 2.

Confidence intervals on the quality of the estimated distributions (the error bars in Fig. 2) have been evaluated as standard deviations of  $G^{(i)}$  as calculated from 40 different Monte Carlo runs. They may appear large, but this is due to the high value of  $G^{(i)}$ , which in turn determines the scale of the plot. Look at panels (d) for comparison.

Finally, we notice that using Eq. (7) for reconstructing the photon distribution we are not taking into account the effects due to the dead time and the dark counts of the detectors. Indeed these effects may be neglected without degrading of the quality of the reconstruction for the following reasons. Dead time is equivalent to an effective reduction of the quantum efficiency, whose amount, however, depends on the state under investigation. Since the state of the detector is under control, we may simply discard the data obtained during the dead time. This procedure only limits the maximum rate of the measurement, which, in our case, may be as fast as 10 MHz. Notice that the relevant parameter is how many times the gate opens and not when it opens during the measurement. The dark counts of our detectors, which are mostly due to thermal noise, are below a few hundreds Hertz. Therefore, by a suitable choice of the measurement gate, they do not influence the counting rate. Of course, if the quantum efficiency is very small, dark counts may influence the statistics. Therefore, we discard the measurements taken at the lower quantum efficiency which, anyway, contain very little information on the state under investigation. In conclusion, dead time and dark counts may be neglected due to the good quality of our detectors which allows reliable measurements with the gate in the range from few hundreds Hertz to some mega Hertz.

#### IV. EXPERIMENTAL DATA

In order to confirm the Monte Carlo results for single-peaked distributions we have performed the reconstruction of the photon statistics of a coherent signal obtained from a Nd:YLF laser. The experimental data have been recorded by a hybrid photodetector, Hamamatsu H8236-40, placed on the second harmonics (523.5 nm) output of a cw mode-locked Nd:YLF laser regeneratively amplified at a repetition rate of 5 kHz (High Q Laser). In Fig. 3 there is the block diagram of the experimental setup.

The frequencies  $f_\nu^m$ , until  $m=3$ , have been extrapolated from the response of the detector with the following procedure. First, a Gaussian best fit of each of the response peaks

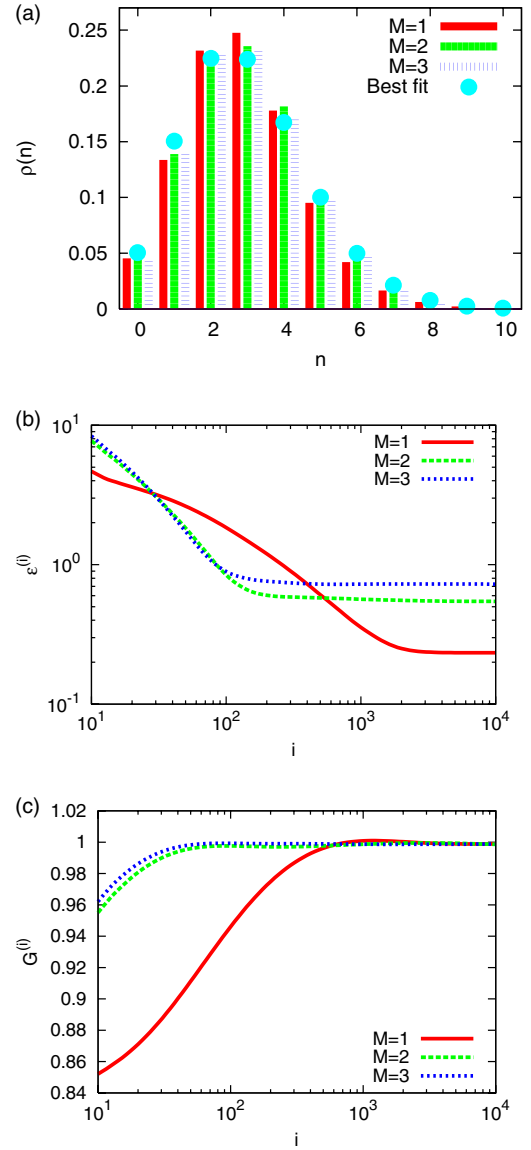


FIG. 4. (Color online) Experimental reconstruction of the photon number distribution of a coherent state. (a) Reconstructed  $p_n$  and coherent best fit,  $\langle a^\dagger a \rangle = 2.98$ ; (b) total absolute error  $\varepsilon^{(i)}$ ; (c) fidelity  $G^{(i)}$  calculated *a posteriori*. The reconstruction is performed with a hybrid photodetector operated by taking  $M=1$  (on/off detector),  $M=2$  and  $M=3$ ;  $K=100$  different quantum efficiencies  $\eta = \eta_\nu$  distributed in  $[0, \eta_{\max}]$ ,  $\eta_{\max} = 0.4$ ; the Hilbert space is truncated at  $N=30$ ;  $n_\nu = 10^4$  number of runs have been performed for each  $\eta$ ; the algorithm is stopped at iteration  $I = n_\nu$ .

corresponding to  $0, \dots, 4$  photoelectrons has been performed [6]. Then, the frequencies have been obtained by choosing three thresholds, whose optimal choice turns out to be the midpoint between photoelectron peaks [24]. Once the frequencies  $f_\nu^m$  had been obtained, we used the algorithm of the preceding section. The results of the reconstruction are shown in Fig. 4, panel (a). The reconstructed distribution at the last iteration  $\varrho_n^{(I)}$  have been then compared with a Poissonian best fit. As it is evident from Fig. 4, the agreement between  $\varrho_n^{(I)}$  and the best fit is very good. In addition, we notice that the shape of  $G^{(i)}$  and  $\varepsilon^{(i)}$  are very similar to those

coming from simulation and that the  $\varrho_n^{(i)}$  obtained from the experimental data with  $M=1$  is close to that obtained with  $M=2$  and  $M=3$ , as predicted by simulations.

## V. CONCLUSION

We have presented a detailed comparison, based on Monte Carlo simulated experiments and real data, among the performances of detectors with different upper limits of counting capability (resolution). We found that using maximum-likelihood methods, detectors with high quantum efficiency does not need to have high counting capability, since on/off detection already provides good reconstructions.

On the other hand, a small quantum efficiency makes the counting capability a crucial parameter. Overall, our results indicate that development of future photodetectors may be focused on increasing the quantum efficiency rather than the counting capability.

## ACKNOWLEDGMENTS

The authors are grateful to Alessandra Andreoni for encouragement and support. They also thank Maria Bondani, Andrea R. Rossi, Fabio Ferri, Zdenek Hradil, and Jarda Řeháček for useful discussions. This work has been supported by MIUR through project Nos. PRIN-2005024254-002 and FIRB-RBAU014CLC-002.

- 
- [1] M. Dakna, J. Clausen, L. Knoll, and D.-G. Welsch, *Phys. Rev. A* **59**, 1658 (1999); M. G. A. Paris, *ibid.* **62**, 033813 (2000); M. G. A. Paris, M. Cola, and R. Bonifacio, *ibid.* **67**, 042104 (2003); J. Laurat, T. Coudreau, N. Treps, A. Maitre, and C. Fabre, *Phys. Rev. Lett.* **91**, 213601 (2003); S. A. Babichev, B. Brezger, and A. I. Lvovsky, *ibid.* **92**, 047903 (2004).
  - [2] E. Knill, R. Laflamme, and G. J. Milburn, *Nature (London)* **409**, 46 (2001).
  - [3] D. Rosenberg, A. E. Lita, A. J. Miller, and S. W. Nam, *Phys. Rev. A* **71**, 061803(R) (2005).
  - [4] R. DeSalvo, *Nucl. Instrum. Methods Phys. Res. A* **387**, 92 (1997).
  - [5] F. Zappa, A. L. Lacaita, S. D. Cova, and P. Lovati, *Opt. Eng.* **35**, 938 (1996); D. Achilles, C. Silberhorn, C. Śliwa, K. Banaszek, and I. A. Walmsley, *Opt. Lett.* **28**, 2387 (2003).
  - [6] G. Zambra, M. Bondani, A. S. Spinelli, F. Paleari, and A. Andreoni, *Rev. Sci. Instrum.* **75**, 2762 (2004).
  - [7] E. Hergert, Single Photon Detector Workshop, NIST, Gaithersburg, 2003.
  - [8] J. Kim, S. Takeuchi, Y. Yamamoto, and H. H. Hogue, *Appl. Phys. Lett.* **74**, 902 (1999); A. Peacock, P. Verhoeve, N. Rando, A. van Dordrecht, B. G. Taylor, C. Erd, M. A. C. Perryman, R. Venn, J. Howlett, D. J. Goldie, J. Lumley, and M. Wallis, *Nature (London)* **381**, 135 (1996).
  - [9] G. Di Giuseppe, A. V. Sergienko, B. E. A. Saleh, and M. C. Teich, in *Quantum Information and Computation*, edited by E. Donkor, A. R. Pirich, and H. E. Brandt [Proc. SPIE 5105, 39 (2003)].
  - [10] M. Munroe, D. Boggavarapu, M. E. Anderson, and M. G. Raymer, *Phys. Rev. A* **52**, R924 (1995); Y. Zhang, K. Kasai, and M. Watanabe, *Opt. Lett.* **27**, 1244 (2002).
  - [11] M. Raymer and M. Beck, in *Quantum States Estimation*, edited by M. G. A. Paris and J. Řeháček, Lecture Notes in Physics Vol. 649 (Springer, Berlin-Heidelberg, 2004).
  - [12] P. L. Kelley and W. H. Kleiner, *Phys. Rev.* **136**, A316 (1964); R. A. Campos, B. E. A. Saleh, and M. C. Teich, *Phys. Rev. A* **40**, 1371 (1989); L. Mandel and E. Wolf, *Optical Coherence and Quantum Optics* (Cambridge University Press, New York, 1995).
  - [13] A. R. Rossi, S. Olivares, and M. G. A. Paris, *Phys. Rev. A* **70**, 055801 (2004).
  - [14] T. Kiss, U. Herzog, and U. Leonhardt, *Phys. Rev. A* **52**, 2433 (1995); G. M. D'Ariano and C. Macchiavello, *ibid.* **57**, 3131 (1998); T. Kiss, U. Herzog, and U. Leonhardt, *ibid.* **57**, 3134 (1998).
  - [15] D. Mogilevtsev, *Opt. Commun.* **156**, 307 (1998); *Acta Phys. Slov.* **49**, 743 (1999).
  - [16] G. Zambra, A. Andreoni, M. Bondani, M. Gramegna, M. Genovese, G. Brida, A. Rossi, and M. G. A. Paris, *Phys. Rev. Lett.* **95**, 063602 (2005).
  - [17] J. Řeháček, Z. Hradil, O. Haderka, J. Peřina, Jr., and M. Hamar, *Phys. Rev. A* **67**, 061801(R) (2003); O. Haderka, M. Hamar, and J. Peřina, *Eur. Phys. J. D* **28**, 149 (2004).
  - [18] H. Paul *et al.*, *Phys. Rev. Lett.* **76**, 2464 (1996).
  - [19] Z. Hradil, *Phys. Rev. A* **55**, R1561 (1997); J. Řeháček, Z. Hradil, and M. Ježek, *ibid.* **63**, 040303 (2001); Z. Hradil, D. Mogilevtsev, and J. Řeháček, *Phys. Rev. Lett.* **96**, 230401 (2006).
  - [20] A. P. Dempster, N. M. Laird, and D. B. Rubin, *J. R. Stat. Soc. Ser. B (Methodol.)* **39**, 1 (1977); Y. Vardi and D. Lee, *ibid.* **55**, 569 (1993).
  - [21] R. A. Boyles, *J. R. Stat. Soc. Ser. B (Methodol.)* **45**, 47 (1983); C. F. J. Wu, *Ann. Stat.* **11**, 95 (1983).
  - [22] K. Banaszek, *Acta Phys. Slov.* **48**, 185 (1998); *Phys. Rev. A* **57**, 5013 (1998).
  - [23] Indeed, we employ the total error rather than the likelihood itself because, besides convergence, it quantifies to which extent the estimated photon number distribution reproduces the experimental data.
  - [24] M. Bondani (unpublished).